A FEATURE-BASED DENSE LOCAL REGISTRATION OF PAIRS OF RETINAL IMAGES

M. Fernandes, Y. Gavet and J. C. Pinoli
Centre Ingénierie et Santé, Ecole Nationale Supérieure des Mines, 158 cours Fauriel, 42023 Saint-Etienne cedex 2, France
Laboratoire des Procédés en Milieux Granulaires (LPMG), UMR CNRS 5148, France

Keywords: Feature-based registration, Retinal images, Opthalmology, Local transformation, Dense transformation.

Abstract: A method for spatial registering pairs of digital images of the retina is presented, using intrinsic feature points (landmarks) and dense local transformation. First, landmarks, i.e. blood vessel bifurcations, are extracted from both retinal images using filtering followed by thinning and branch point analysis. Correspondances are found by topological and structural comparisons between both retinal networks. From this set of matching points, a displacement field is computed and, finally, one of the two images is transformed. Due to complex retinal registration problem, the presented transformation is dense, local and adaptive. Expermimental results established the effectiveness and the interest of the dense registration method.

1 INTRODUCTION

The problem of image registration is fundamental to many applications of computer vision. Solving this problem requires estimating transformation(s) between images and applying them in order to place the data in a common coordinate system (Zitova and Flusser, 2003). In retinal imaging (Figure 1), disease diagnosis and treatment planning are facilitated by multiple spatial images acquired from the same patient. Spatial registration techniques allow to integrate informations into a comprehensive single image. They are typically classified as feature-based or area-based.

In area-based techniques, a similarity measure quantifies the matching between images under an assumption of global transformation and is generally optimized with global search algorithms (Ritter et al., 1999). There are many factors that may degrade the performance of area-based methods: large textureless regions, nonconsistent contrast and nonuniform illumination within images.

Feature-based methods focus on aligning extracted features of the images, i.e bifurcations of the retinal vasculature. From landmarks between both images and with the assumption of correspondances, a global transformation is estimated. These methods are usually more reliable and faster in the case of sufficient and accurate landmarks but a global transformation is always applied. Indeed, image distorsions and aberrations come from different sources:

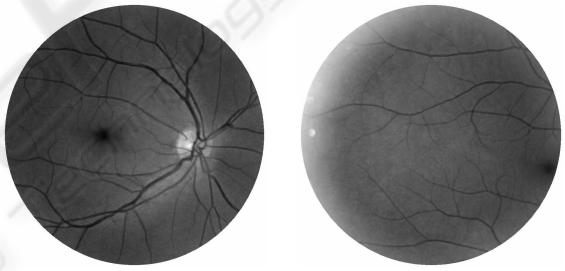

Figure 1: Pair of retinal images of size 924×912 pixels.

- changes in head posture and eye movements,
- projection of the retinal surface on the camera plane,
- optical systems (camera, cornea and crystalline),
- eye deformations due to defects and diseases.

In order to obtain an accurate registration, a global transformation must consider all this considerations with a limited overlapping regions between images. This is why this problem requires intuitively an adaptive local dense approach.

First, the developed feature-based technique using a dense local transformation will be described. Next, we will discuss the results obtained. Finally, conclusions and possible extensions will be given.

Fernandes M., Gavet Y. and Pinoli J. (2009).
A FEATURE-BASED DENSE LOCAL REGISTRATION OF PAIRS OF RETINAL IMAGES.
In *Proceedings of the Fourth International Conference on Computer Vision Theory and Applications*, pages 265-268
DOI: 10.5220/0001797102650268

(a) (b) (c) (d) (e)

Figure 2: (a) Part of a retinal image. (b) Result of morphological contrast and median filter. (c) Result of matched filters, thresholding and cleaning. (d) Thinned and pruned binary image. (e) Detected landmarks (white dots).

2 FEATURE-BASED TECHNIQUE

A feature-based registration method is made of three main steps: landmarks extraction, matching between landmarks and image transformation.

2.1 Landmarks Extraction

Traditionnally, bifurcations are extracted automatically by a retinal vessels segmentation, followed by thinning and branch point analysis. For example, Zana and Klein (Zana and Klein, 1999) enhanced vessels with a sum of top-hats with linear revolving structuring elements and detected bifurcations using a supremum of openings with revolving structuring elements with T shape. In (Becker et al., 1998), the boundaries of retinal vessels are detected using standard Sobel filter and the vasculature is thickened using a minimum filter.

Proposed Methods. Retinal vessels can be approximated by a succession of linear segments (of length L) at different orientations. Afterwards, all used parameter values are experimetal. First, retinal vessels are emphasized using a minimum of morphological contrasts with linear ($L = 9$ pixels) and revolving (30° increments) structuring elements. A median filter smoothed the result image (Figure 2.b). Second, retinal vessels, whose cross section can be approximated by a Gaussian shaped curve (standard deviation σ), are detected by matched filters with 6 orientations, and with $L = 9$ pixels and $\sigma = 2$ (Chaudhuri et al., 1989). Next, the thresholded image is cleaned: small objects (≤ 200 pixels) and small holes (≤ 15 pixels) are deleted (Figure 2.c). Third, the centreline of the vascular tree is obtained with a thinning operation and is pruned so as to eliminate small branches (≤ 15 pixels) (Figure 2.d). Fourth, bifurcations are extracted as skeleton pixels with at least six binary transitions between adjacent pixels of V8 or V16 neighbourhoods. Finally, adjacent and closer landmarks (≤ 10 pixels) are joined: the new landmark corresponds to the centre of mass of the system with equal weights and may not belong to the skeleton (Figure 2.e).

2.2 Landmarks Matching

After extraction, pairs of matching landmarks need to be determined between both images. (Can et al., 2002) and (Zana and Klein, 1999) suggested similarity measures between bifurcations depending on surrounding vessels angles. Due to nonuniform illuminations, a similarity measure may not be robust. (Becker et al., 1998) and (Ryan et al., 2004) computed simple transformation parameters from all possible combinations of landmarks. From this data set, matched landmark pairs form a tight cluster which is unfortunately demarcated with difficulty.

Proposed Methods. Let I_p and I_q denote both images called arbitrarily reference and transformed image respectively and with $\mathcal{P}$ and $\mathcal{Q}$ extracted landmark sets respectively. (u,v) and (u',v') are the coordinates systems of I_p and I_q respectively. In this paper, the matching technique proceeds in two steps.

The first step is a similarity measure between landmark signatures of both images and results in an initial couples set $\mathcal{S}$. For a landmark p, the signature is the number of surrounding vessels n_p and the angles between them $\theta_{p_1},\cdots,\theta_{p_{n_p}}$ obtained by computing the intersection between the pruned skeleton and a circle of fixed diameter $o = 24$ pixels centred on it. For each (p,q) belonging to $\mathcal{P}\times\mathcal{Q}$, (p,q) belongs to $\mathcal{S}$ if and only if $n = n_p = n_q \leq 5$ and $\theta_{q_i} - \alpha \leq \theta_{p_i} \leq \theta_{q_i} + \alpha$ for $i = 1,\cdots,n$ and with $\alpha = 10^\circ$. This step restricts landmarks sets $\mathcal{P}$ and $\mathcal{Q}$ before the second step which is more time consuming.

The second step consists in estimating, for each initial couple, the spatial agencement of landmarks between the two images (Figure 3). For an initial couple (p_{S_j}, q_{S_j}) belonging to $\mathcal{S}$, whose locations (u_{S_j}, v_{S_j}) and (u'_{S_j}, v'_{S_j}) constitute now images origins, landmarks from the two images that have the same locations with a given tolerance value δ are preserved :

$$\mathcal{C}_j = \left\{ \begin{array}{c} (p,q) \in \mathcal{P}\times\mathcal{Q} \mid q = (u',v') \\ \in [u'_{S_j} + \Delta u - \delta\,;\, u'_{S_j} + \Delta u + \delta] \\ \times [v'_{S_j} + \Delta v - \delta\,;\, v'_{S_j} + \Delta v + \delta] \end{array} \right\}, \quad (1)$$

with $\Delta u = u - u_{S_j}$, $\Delta v = v - v_{S_j}$, $p = (u,v)$ and $\delta = 8$ pixels. The final matching set $\mathcal{C}$ corresponds to the

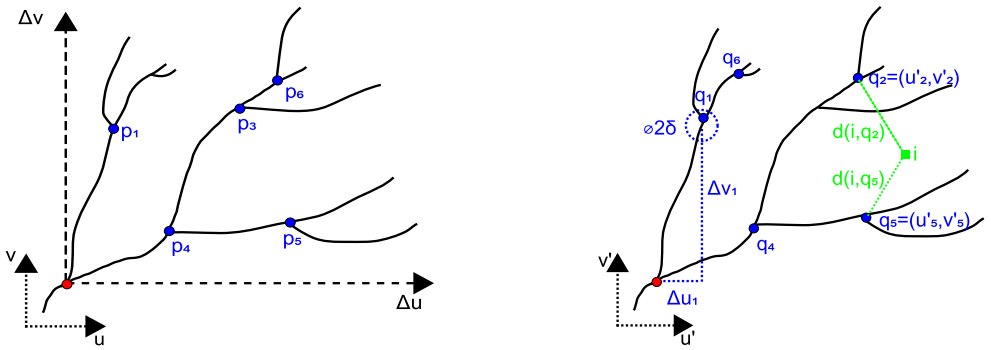

(a) Reference image I_p (b) Transformed image I_q

Figure 3: Illustrating the second point matching step and the displacement vector computation. Red dots indicate one initial couple belonging to $\mathcal{S}$. Blue dots indicate the others landmarks belonging to $\mathcal{P}$ or to $\mathcal{Q}$. All landmarks locations of I_p are verified in I_q with a given tolerance distance δ. Initial couple, pairs 1, 2, 4 and 5 are preserved and landmarks p_3 and q_6 are eliminated. For the displacement vector computation, 2 and 5 are the two nearest preserved pairs of the pixel i of I_q.

best spatial agencement similarity set:

$$\mathcal{C} = \mathcal{C}_{\text{argmax}_{j=1,\cdots,card\,\mathcal{S}}\, card(\mathcal{C}_j)} \,. \tag{2}$$

This step increases reliable matching and robustness.

2.3 Image Transformation

Having established landmark matchings, the next task is to identify a suitable transformation. All cited references employed global linear or not transformations. According to (Becker et al., 1998), the affine model is appropriate because the retina is roughly planar over small regions and, consequently, parallel with the camera plane. In (Can et al., 2002), the retina is modelled by a quadratic surface, the camera movements by rigid transformations and the projections on the camera plane by weak perspective projections. The resulting quadratic transformation have 12 parameters. However, the difficult problem of spatial retinal registration leads to produce local adaptive deformations and motivates the following transformation.

Proposed Methods. To match I_p, a dense displacement vector field, function of $\mathcal{C}$, locally deforms I_q. For one pixel i of I_q, first, the two nearest couples belonging to $\mathcal{C}$ are sought:

$$(p_1,q_1) = \underset{(p_C,q_C)\in\mathcal{C}}{\text{argmin}}\; d(i,q_C) \tag{3}$$

$$(p_2,q_2) = \underset{(p_C,q_C)\in\mathcal{C}-\{(p_1,q_1)\}}{\text{argmin}}\; d(i,q_C)\,, \tag{4}$$

with d the Euclidean distance defined on the spatial support of I_q (Figure 3). Then, the distinct displacement vector of i is:

$$\overrightarrow{T_i} = \begin{pmatrix} \frac{1/d(i,q_1).(u_1-u'_1)+1/d(i,q_2).(u_2-u'_2)}{1/d(i,q_1)+1/d(i,q_2)} \\ \frac{1/d(i,q_1).(v_1-v'_1)+1/d(i,q_2).(v_2-v'_2)}{1/d(i,q_1)+1/d(i,q_2)} \end{pmatrix}, \tag{5}$$

with $p_1=(u_1,v_1)$, $q_1=(u'_1,v'_1)$, $p_2=(u_2,v_2)$ and $q_2=(u'_2,v'_2)$.

When all pixels of I_q are computed, a dense displacement vector field is obtained which is regularized using a Gaussian filter. Finally, I_q is transformed: the mapped positions of pixels is calculated as the sum of their original locations and their corresponding displacement vectors.

3 RESULTS

All visible bifurcations are globally extracted except ones belonging to very narrow vessels due to the unscalability of used matched filters. The matching process is able to match landmarks with large coordinates differences between images (typically the case of a spatial registration) and, intrinsically, to obtain correspondances which are very rarely incorrect.

In this paper, visual assessment on the fused image between reference and transformed images is adopted. With limited overlapping regions (typically the case of spatial registration), i.e with few matching landmarks, the dense local registration outperforms the quadratic model estimated using linear regression (Laliberte et al., 2003) (Ryan et al., 2004) (Figure 4). The quadratic model estimated using linear regression needs larger number of matching landmarks in order to obtain conveniently optimal parameters estimation and to achieve an accurate result. However, both registration methods are affected by the lack of matching

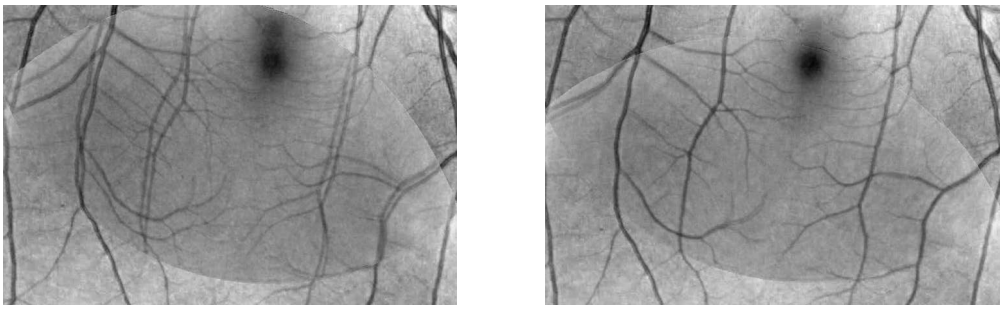

(a) Quadratic transformation (b) Dense local transformation

Figure 4: Overlapping regions of registration for a pair of images (Figure 1) and with 15 extracted matching couples.

informations in some areas. Therefore, in the case of the presented dense local registration, vessel misalignments appear in some peripheral areas.

4 CONCLUSIONS

In this paper, we have described a feature-based, dense, local registration for eye fundus images. This method is efficient and avoids iterations or heavy calculations. It allows to cope with complex recognitions of global transformation. On the one hand, it avoids high-order global transformation due to complex retinal registration problem. On the other hand, obtaining conveniently optimal parameters with few matching landmarks is a difficult task due to limited overlapping regions of spatial registration.

In order to minimize misalignments due to the lack of intrinsic landmarks uniformity, we are currently investigating the use of additional regional landmarks like the whole vessels. We are also developing a protocol so as to quantitatively compare different registration processes.

ACKNOWLEDGEMENTS

The authors wish to thank Pr. Gain from University Hospital Centre, Saint-Etienne, France for supporting this work and for providing pictures.

REFERENCES

Becker, D., Can, A., Turner, J., Tanenbaum, H., and Roysam, B. (1998). Image processing algorithms for retinal montage synthesis, mapping, and real-time location determination. *IEEE Transactions on Biomedical Engineering*, 45(1):105–118.

Can, A., Stewart, C., Roysam, B., and Tanenbaum, H. (2002). A feature-based, robust, hierarchical algorithm for registering pairs of images of the curved human retina. *IEEE Transactions on Pattern Analysis and Machine Intelligence*, 24(3):347–364.

Chaudhuri, S., Chatterjee, S., Katz, N., Nelson, M., and Goldbaum, M. (1989). Detection of blood vessels in retinal images using two-dimensional matched filters. *IEEE Transactions on Medical Imaging*, 8(3):263–269.

Laliberte, F., Gagnon, L., and Sheng, Y. (2003). Registration and fusion of retinal images - an evaluation study. *IEEE Transactions on Medical Imaging*, 22(5):661–673.

Ritter, N., Owens, R., Cooper, J., Eikelboom, R., and Van Saarloos, P. (1999). Registration of stereo and temporal images of the retina. *IEEE Transactions on Medical Imaging*, 18(5):404–418.

Ryan, N., Heneghan, C., and de Chazal, P. (2004). Registration of digital retinal images using landmark correspondence by expectation maximization. *Image and Vision Computing*, 22(11):883–898.

Zana, F. and Klein, J. (1999). A multimodal registration algorithm of eye fundus images using vessels detection and hough transform. *IEEE Transactions on Medical Imaging*, 18(5):419–428.

Zitova, B. and Flusser, J. (2003). Image registration methods: a survey. *Image and Vision Computing*, 21(11):977–1000.